Poly(ethylene-*co*-vinyl alcohol) and Nylon 6/12 Nanofibers Produced by Melt Electrospinning System Equipped with a Line-Like Laser Beam Melting Device

Naoki Shimada, Hideaki Tsutsumi, Koji Nakane, Takashi Ogihara, Nobuo Ogata

Department of Materials Science and Engineering, University of Fukui, 3-9-1 Bunkyo, Fukui 910-8507, Japan

Received 8 April 2009; accepted 19 November 2009
DOI 10.1002/app.31837
Published online 4 February 2010 in Wiley InterScience (www.interscience.wiley.com).

ABSTRACT: A new melt electrospinning system equipped with a line-like laser beam melting device developed for the mass production of nanofibers is introduced; this system enables fibers to be produced from locally melted polymer sheets in the presence of an electric field. Using this system, fibers were produced from poly(ethylene-*co*-vinyl alcohol)(EVOH) and Nylon 6/12 sheets. The fiber formation mechanism was investigated with a video camera and a thermographic camera. It was found that (1) many Taylor cones are formed on the molten end surface of the sheet at almost regular intervals; (2) a single fiber is produced from the apex of each Taylor cone; and (3) the temperature in the Taylor cone changes markedly during the fiber production. Furthermore, it is found that fibers with an average diameter smaller than 1 μm can be produced from EVOH and Nylon 6/12 sheets by the optimization of manufacturing parameters such as laser output power, voltage, sheet thickness and the feed rate of the sheet. © 2010 Wiley Periodicals, Inc. J Appl Polym Sci 116: 2998–3004, 2010

Key words: melt electrospinning; line-like laser beam; EVOH; nylon 6/12

INTRODUCTION

Recently, various engineering fields have devoted a great deal of attention to nanoscale materials. In the fiber industry, nanofibers have been the object of this attention. Such fibers are potentially useful in a variety of engineering applications in which a large surface area and fibrous structure are demanded.[1–3] Electrospinning is a simple technique for the production of nanofibers that can be classified into two kinds of methods: solvent electrospinning methods and melt electrospinning methods. Although solvent electrospinning methods have solvent recycling issues and low productivity, studies using these methods abound because the setup is inexpensive and simple. Melt electrospinning methods eliminate the issues related to solvents, and thus melt electrospinning is considered to be a more ecofriendly, versatile, and low-cost production method.[4–6] However, there are few studies on melt electrospinning because this process does not include fiber thinning which occurs as a result of solvent evaporation during solvent electrospinning.

We previously developed a melt electrospinning system with a spot-like laser beam melting device. A rod-like polymer material was prepared, the tip of the rod was irradiated by a spot-like laser beam, the tip was melted and a high voltage was applied between the melted part and the collector, forming a Taylor cone from which a nanofiber was drawn. We obtained nanofibers from several different polymers using this system,[7–11] called "spot laser melt electrospinning." A major problem with this system is that the fiber productivity is low because only a single nanofiber is produced from the rod. To solve that problem, we have developed a new melt electrospinning system which can produce nanofibers in bulk not from a rod but from a polymer sheet. The basic idea of our melt electrospinning method is as follows. The line melted zone is produced at the end of the polymer sheet by irradiating a line-like laser beam. If many Taylor cones, which are the origin of nanofibers, are formed simultaneously on the melted zone, the fiber productivity would increase. However, the formation of Taylor cone from the line melted zone has not been investigated. As samples, we selected poly(ethylene-*co*-vinyl alcohol) (EVOH) and Nylon 6/12 sheets because nanofibers had been successfully produced from these materials in the rod-based method; the samples were the same used in the previous work.[7]

In this work, a new electrospinning system equipped with a line-like laser beam melting device is introduced, and called "line laser melt electrospinning". Here, we describe the formation process of fibers in this method and report the production of fibers from EVOH and Nylon 6/12 sheets and the

Correspondence to: N. Ogata (ogata@matse.u-fukui.ac.jp).

effects of production conditions on the fiber diameter.

EXPERIMENTAL

Materials

Poly(ethylene-*co*-vinyl alcohol)(EVOH) and Poly (hexamethylene dodecanediamide) (Nylon 6/12) were selected as spinning materials. Pellet-like EVOH (#F104B) was supplied by Kuraray (Osaka, Japan). The characterization of the pellets is as follows: ethylene content = 32 mol %, T_m = 183°C, *MFI* = 4.4 (190°C, 21.2N). Pellet-like Nylon 6/12 was purchased from Aldrich. The pellets had the following characteristics: T_m = 218°C, T_g = 46°C, density 1.3 g/mL at 25°C. Sheets (150 × 100 mm^2) with thicknesses of 0.5 mm, 0.75 mm, and 1.0 mm were produced by the melt press of these pellets. The temperatures used for the melt press of EVOH and Nylon 6/12 were 200 and 230°C, respectively. The resultant sheets were used for the melt electrospinning tests.

Melt-electrospinning system

A line-like laser beam was generated from a spot-like CO_2 laser beam generator (Universal Laser System, ULR-50, φ4 mm, nominal output power = 50 W, wave length = 10.6 μm, USA) using a custom-built optical system; the line-like laser beam was designed to show a top-hat-shaped uniform output intensity distribution over 150 mm in length and less than 2 mm in width. The optical system consists of three mirrors, a laser beam homogenizer, a collimator lens, a cylindrical convex lens and a cylindrical concave lens. To identify the intensity distribution of the line-like laser beam, a poly(methylmethacrylate) (PMMA) board 8 mm in thickness was set at the focal point of the convex lens and engraved by the laser beam at a maximum output power (61 W); the engraved form exhibits the intensity distribution of the laser beam. Figure 1 shows the intensity distribution of the beam used to irradiate the polymer sheets. Contrary to our expectation, we could not obtain a top-hat-shaped uniform laser output intensity distribution over 150 mm in length; the thickness of the line-like laser was about 1.4 mm. Figure 2 shows a schematic diagram of the main part of the melt electrospinning system invented in this work. A sheet sample was fed to the line laser melting zone at a feed rate (F_r) of 0.05 to 1 mm/s. One end of the sheet was locally and linearly melted by the laser beam. High voltage was applied to the linearly melted zone through a copper slit; the minimum length between the edge of the copper slit and the line laser was 5 mm. The fibers produced could be collected onto the copper anode collector plate (100 × 100 × 2 mm^3).

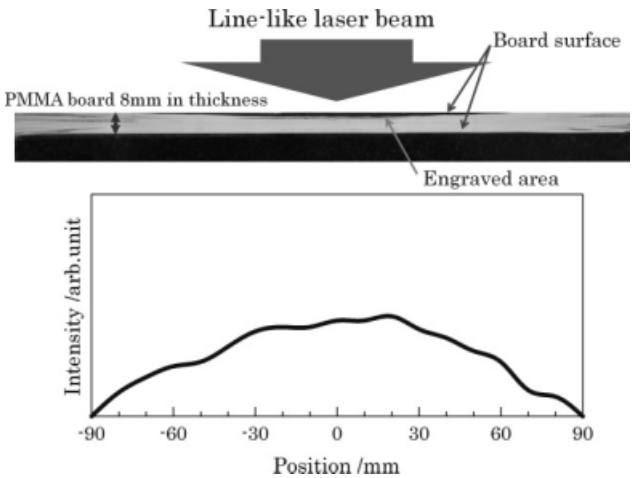

Figure 1 Laser intensity profile used in this work.

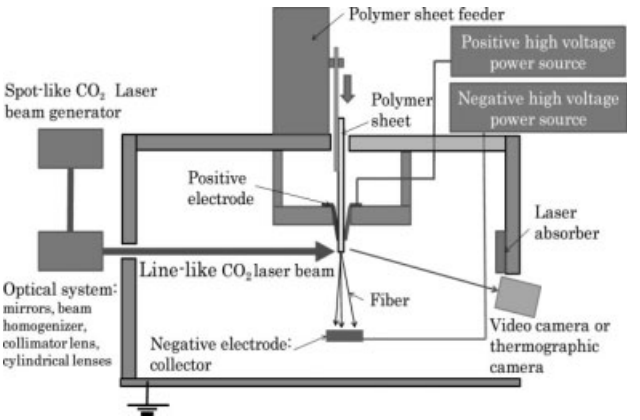

Figure 2 Schematic diagram of the line laser melt electrospinning system used in this work.

Melt-electrospinning conditions

Voltage was applied between the copper slit and the collector, and its maximum value was 120 kV (two high voltage power suppliers +60 kV and −60 kV were used); the voltage (H_v) was 40 kV unless otherwise noted. The laser power (L_p) used represents the power of the laser beam when launched from the spot-like laser beam generator and measured with a laser power meter; it was 45.0 W unless otherwise noted. The molten end-to-collector distance, or the "collector distance" (C_d), was 100 mm unless otherwise noted.

Observation of fiber formation process

The fiber formation process was observed with a high definition video camera (Canon, iVIS HV20, Japan). The temperature of the linearly melting zone was measured using a thermographic camera (Apiste, FSV-7000E, Osaka, Japan) with a notch filter,

which prevented scattered laser light (wavelength 10.6 μm) from entering the camera.

Characterization of fibers

The morphology of the electrospun fibers was examined with a Keyence scanning electron microscope (SEM, VE-9800, Kyoto, Japan). Since a top-hat-shaped uniform laser output intensity distribution was not obtained, we examined the electrospun fibers formed from the central portion of the laser distribution. The fiber samples were gold-sputter coated with an ion coater (Sanyuudensi, SC-701, Tokyo, Japan) as a previous treatment. The average fiber diameter and standard deviation were determined from 50 measurements of fibers obtained for each spinning condition using an Adobe Photoshop CS3 extended program; the average diameter and its standard deviation are referred to as D and σ, respectively.

RESULTS AND DISCUSSION

Formation of the Taylor cones

It is found that the melt electrospinning system with a line-like laser melting device enables many Taylor cones to be simultaneously formed from a line melted zone. As this melt electrospinning system with a line-like laser melting device is a new invention, its fiber formation mechanism is unknown. To clarify our understanding of the mechanism, we observed the morphology of the fibers with a video camera. The observed results are as follows. When the polymer sheet was melted by the laser beam in the presence of high voltage, wave-like perturbations, or meniscus instability, took place on the surface of the molten polymer and then these developed into Taylor cones. From the tip of each Taylor cone, only a single fiber would be spun toward the collector; we could not record it on the photograph because its fiber diameter was so small.

The formation of fibers was accompanied by the generation of fine bubbles in the Taylor cones and gas formation. The surface of the Taylor cone formed from Nylon 6/12 had a greater tendency to become black than that formed from EVOH because Nylon 6/12 was markedly carbonized. Once a Taylor cone was well-formed, its position did not change. However, undeveloped Taylor cones disappeared and the cones were newly formed at another melted surface. The fiber production seems to increase as the Taylor cones developed.

Fiber formation processes from EVOH and Nylon 6/12 sheets were observed with a video camera. Figure 3 shows the effect of the sheet thickness (T) of EVOH on the formation of the Taylor cone. The upper area of the photograph is the positive electrode attached to a scale. The central white area is the unmelted sheet and the dark colored area is the melted area (width *ca.* 1.5 mm). Many Taylor cones can be seen on the surface of the melted area. It should be noted that the length between Taylor cones is almost constant (*ca.* 5 mm), although the laser has a wide intensity distribution (see Fig.1). This result suggests that the there is a static electric repulsion between the cones. As the length between Taylor cones was considered to be a determining factor of the uniformity of the fiber mats produced, we measured the length. When the Taylor cones were undeveloped, the distances between the apexes of wave-like perturbation were measured; the length is referred to as L_t. The meniscus instability can be seen on the $T = 0.5$ mm sheet. Well developed Taylor cones can be seen on the $T = 1.0$ mm sheet. This result means that a sufficient amount of molten polymers is necessary to develop the cone. The value of L_t of the $T = 1.0$ mm sheet seems to be larger than that of the $T = 0.5$ mm sheet. This result suggests that the value of L_t would be determined by the electrostatic repulsion of the Taylor cones. Anyway, it should be noted that the length between Taylor cones is 4–6 mm. The effect of the sheet thickness of Nylon 6/12 on the formation of the Taylor cone was also investigated. The results were similar to those obtained on EVOH and the value of L_t was 5–8 mm.

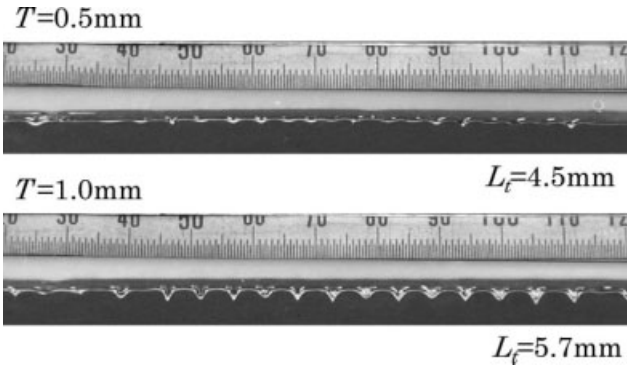

Figure 3 Effect of EVOH sheet thickness, T, on the formation of the Taylor cone; $F_r = 1.0$ mm/min, $C_d = 114$ mm.

Figure 4 shows the effect of the feed rate (F_r) of the sheet of EVOH on the formation of Taylor cones. At a low feed rate ($F_r = 0.25$ mm/min), well developed Taylor cones cannot be seen. However, well developed Taylor cones can be seen at $F_r = 1.0$ mm/min, and L_t seems to increase from 5.5 mm to 7.9 mm with increasing F_r. This result means that the increase in F_r and the increase in T provide the same effect on the formation of Taylor cones.

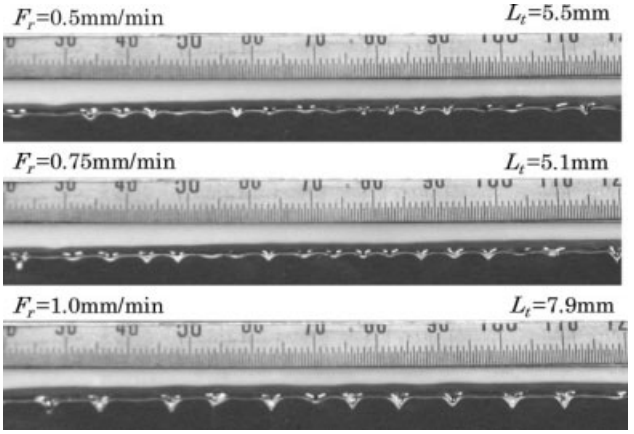

Figure 4 Effect of EVOH sheet feed rate, F_r, on the formation of the Taylor cone; $T = 0.75$ mm, $C_d = 114$ mm.

Thermographic analysis of melting zone

The temperature of the linearly melting zone was measured with a thermographic camera. It was found that the temperature at any point in the linearly melting zone changes over time. We set the center line perpendicular to the linearly melting zone and parallel to the sheet feeding direction. Along this center line, four pixels, P_1, P_2, P_3, and P_4, were defined from the tip of the Taylor cone in an upward direction; the interval between pixels was about 1mm. That is, P_1 is the point in the vicinity of the Taylor cone, P_4 is the point in the vicinity of the unmelted area. Figure 5 shows the temperature variation of each point of the EVOH sheet with time. The temperatures measured at P_3 and P_4 become constant with time; the temperature measured at P_4 is reasonably lower than that measured at P_3. However, it can be seen that the temperature at P_2 has a mean value but changes markedly in the range from 220 to 600°C around the mean value with time. Considering these temperature changes and the fact that gas is generated and bubbles are formed during the fiber formation process, we can say at least that the fiber formation is accompanied by marked temperature changes in the vicinity of the Taylor cone. The experiment was also performed on Nylon 6/12. A similar result was obtained, and its temperature variation was even more marked than that of EVOH.

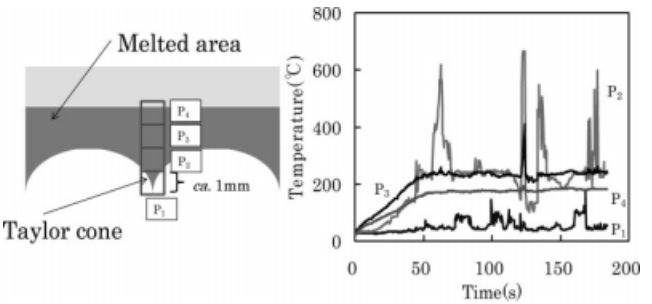

Figure 5 Temperature variation of each point of EVOH sheet with time; $T = 0.75$ mm, $F_r = 1.0$ mm/min.

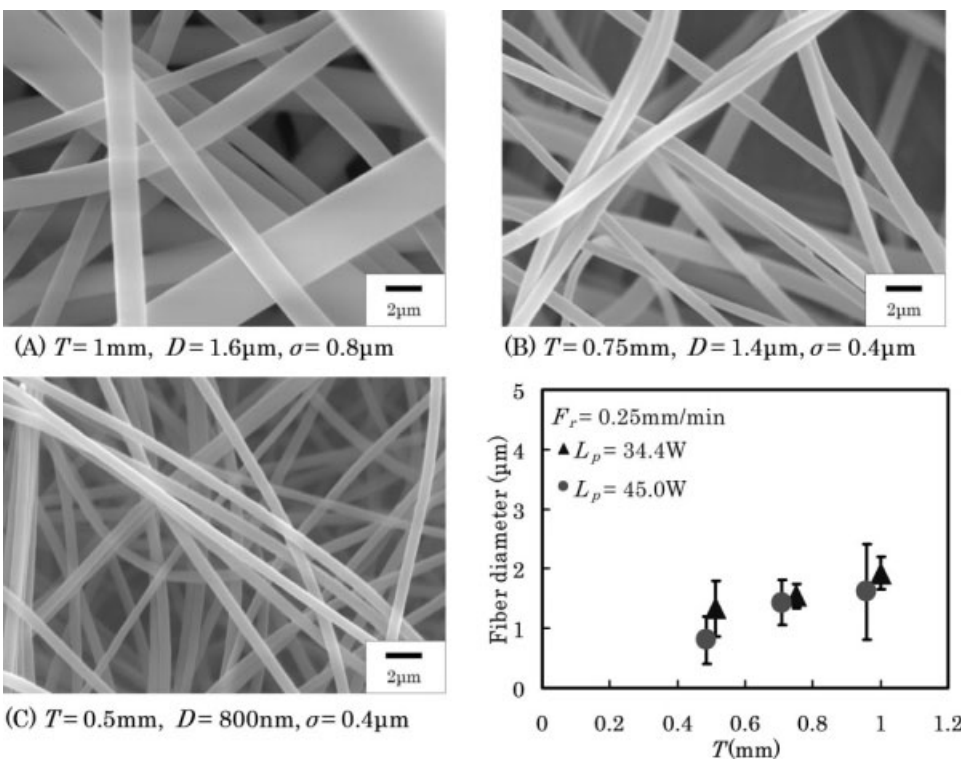

Figure 6 Effect of the sheet thickness, T, of EVOH on the diameter of fibers produced; $F_r = 0.25$ mm/min.

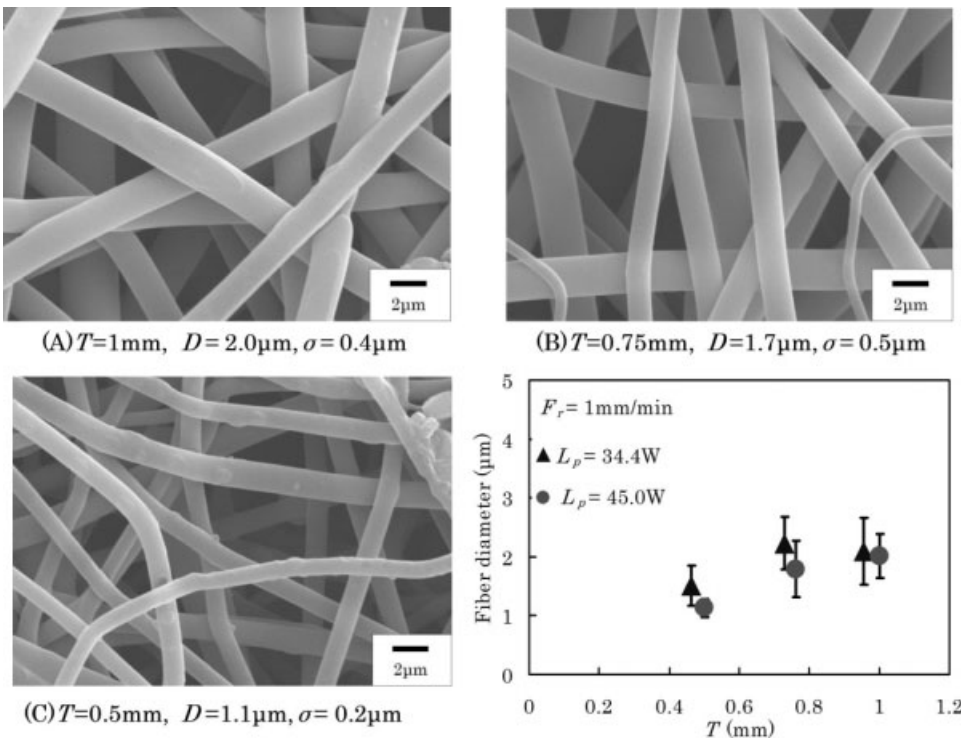

Figure 7 Effect of the sheet thickness, T, of Nylon 6/12 on the diameter of fibers produced; $F_r = 1.0$ mm/min.

Effect of processing parameters on fiber diameter

Figure 6 shows the effect of the sheet thickness (T) of EVOH on the diameter of fibers produced. It can be seen that the average fiber diameter increases with increasing T. Furthermore, an increase in laser output power, L_p, seems to decrease the average fiber diameter. It should be noted that fibers with an average diameter under 1 μm can be obtained by the selection of adequate manufacturing conditions.

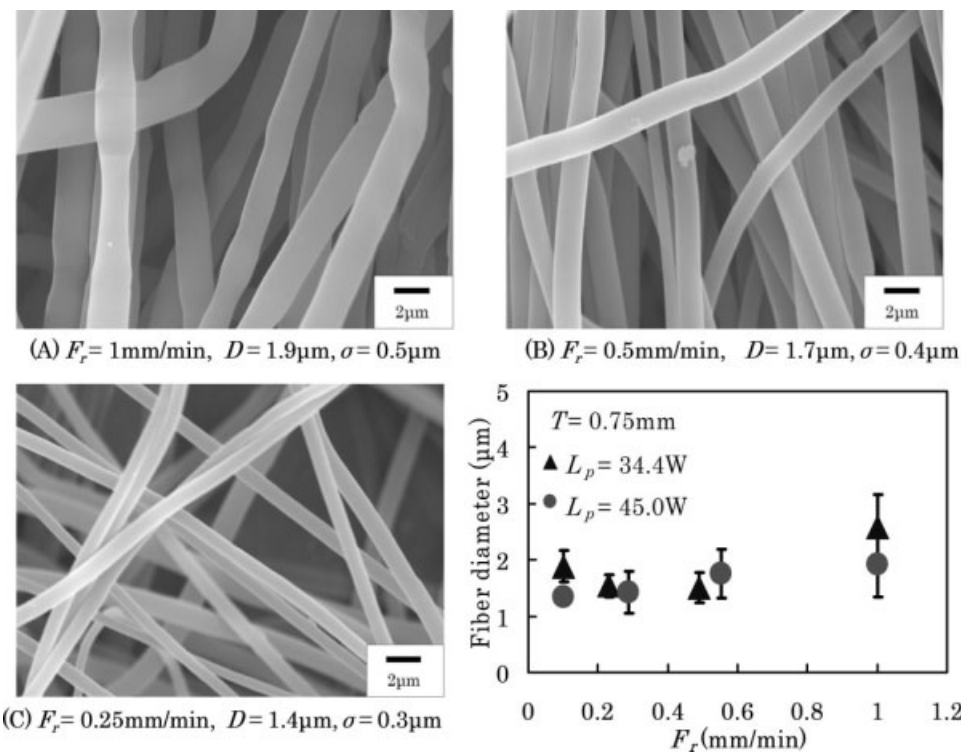

Figure 8 Effect of the feed rate, F_r, of EVOH sheet on the fiber diameter produced; $T = 0.75$ mm.

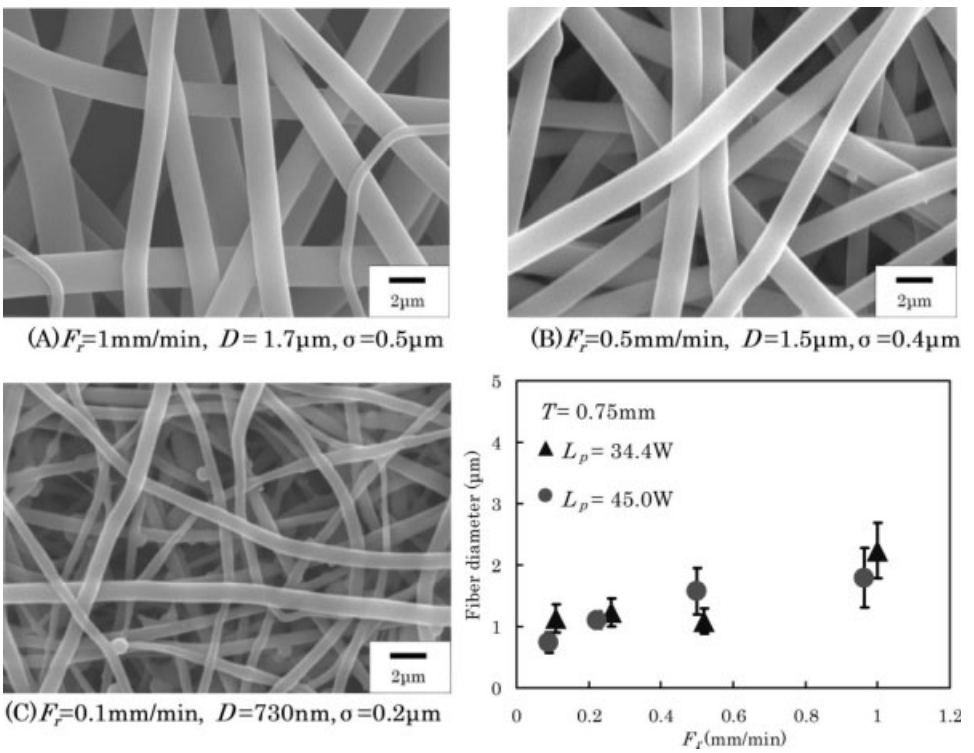

Figure 9 Effect of the feed rate, F_r, of Nylon 6/12 sheet on the fiber diameter produced; $T = 0.75$ mm.

Figure 7 shows the effect of T of Nylon 6/12 on the fiber diameter. It can be seen that the average fiber diameter increases with increasing T. The effect of T on the fiber diameter appears to be independent of the kind of polymer sheet used.

Figure 8 shows the effect of the feed rate (F_r) of the EVOH sheet on the fiber diameter produced. As can be seen, the average fiber diameter increases as the value of F_r increases. The dependence of the laser output power on the average fiber diameter is not clear. Figure 9 shows the effect of F_r of a Nylon 6/12 sheet on the fiber diameter produced. As with the EVOH sheet, the average fiber diameter increases as the value of F_r increases.

From these results, we can say that the fiber diameter deceases with decreasing feed rate of polymer sheets.

Our previous work showed that, in spot laser melt electrospinning, the average fiber diameter decreased as the feed rate of rod-like polymer increased.[10] Therefore, the spinning process of the line laser melt electrospinning appears to differ from that of spot laser melt electrospinning. Figure 10 shows the appearance of melts formed during the melt electrospinning process. A fusiform-shaped melt is formed during the spot laser melt electrospinning of a rod-like polymer material. On the other hand, during the line laser melt electrospinning of polymer sheet, the melt consists of a band-like area and cone-like area; the lateral surface of the cones is concave due to the static electric repulsion between them. The feed of the melts to generate fiber appears to be more complex in line laser melting than in spot laser melting. The difference of the shape of the melts would be responsible for the differences of the dependence of the feed rate of the sample on the fiber diameter. However, this is not clear in this work.

The Taylor cones develop well, and the average fiber diameter increases with increasing T and F_r. That is, it seems that there is a trade-off relation between the average fiber diameter and the amount of fibers produced because the amount increases with the development of the Taylor cones.

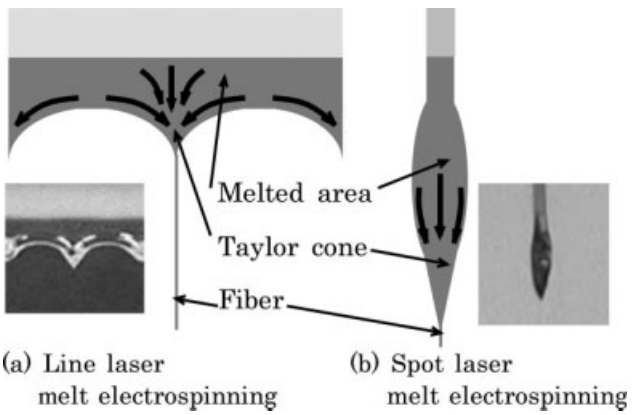

Figure 10 Flow of molten polymers during the laser melt electrospinning process.

CONCLUSIONS

A new melt electrospinning system equipped with a line-like laser beam melting device was developed with the aim of mass producing nanofibers. Using the new system, we produced fibers from EVOH and Nylon 6/12 sheets and observed the fiber formation process. The following conclusions were reached.

1. Taylor cones are formed at almost constant intervals on the melting surface of EVOH and Nylon 6/12.
2. The formation of fibers is accompanied by large temperature changes.
3. EVOH and Nylon 6/12 fibers having an average fiber diameter smaller than 1 μm can be produced from the invented spinning system.
4. The average fiber diameter of EVOH and Nylon 6/12 decreases as the sheet thickness and/or feed rate of the sheet decrease.

References

1. Huang, Z.-M.; Zhang, Y.-Z.; Kotaki, M.; Ramakrishna, S. Compos Sci Technol 2003, 63, 2223.
2. Chronakis, I. S. J Mater Process Tech 2005, 167, 283.
3. Nasir, M.; Matsumoto, H.; Danno, T.; Minagawa, M.; Irisawa, T.; Shioya, M.; Tanioka, A. J Polym Sci Part B: Polym Phys 2006, 44, 779.
4. Lyons, J.; Li, C.; Ko, F. Polymer 2004, 45, 7597.
5. Zhou, H.; Green, T. B.; Joo, Y. L. Polymer 2006, 47, 7497.
6. Dalton, P. D.; Grafahrend, D.; Klinkhammer, K.; Klee, D.; Möller, M. Polymer 2007, 48, 6823.
7. Ogata, N.; Lu, G.; Iwata, T.; Yamaguchi, S.; Nakane, K.; Ogihara, T. J Appl Polym Sci 2007, 104, 1368.
8. Ogata, N.; Yamaguchi, S.; Shimada, N.; Lu, G.; Iwata, T.; Nakane, K.; Ogihara, T. J Appl Polym Sci 2007, 104, 1640.
9. Ogata, N.; Shimada, N.; Yamaguchi, S.; Nakane, K.; Ogihara, T. J Appl Polym Sci 2007, 105, 1127.
10. Shimada, N.; Ogata, N.; Miyashita, H.; Nakane, K.; Ogihara, T. J Text Eng 2008, 54, 143.
11. Tian, S.; Ogata, N.; Shimada, N.; Nakane, K.; Ogihara, T.; Yu, M. J Appl Polym Sci 2009, 113, 1282.